PROCEEDINGS OF SPIE

SPIEDigitalLibrary.org/conference-proceedings-of-spie

Aerogel scattering filters for cosmic microwave background observations

Thomas Essinger-Hileman, Charles L. Bennett, Lance Corbett, Haiquan Guo, Tobias Marriage, et al.

Thomas Essinger-Hileman, Charles L. Bennett, Lance Corbett, Haiquan Guo, Tobias Marriage, Mary Ann B. Meador, Karwan Rostem, Edward J. Wollack, "Aerogel scattering filters for cosmic microwave background observations," Proc. SPIE 10708, Millimeter, Submillimeter, and Far-Infrared Detectors and Instrumentation for Astronomy IX, 107080F (9 July 2018); doi: 10.1117/12.2313387

SPIE.

Event: SPIE Astronomical Telescopes + Instrumentation, 2018, Austin, Texas, United States

Aerogel scattering filters for cosmic microwave background observations

Thomas Essinger-Hileman[a], Charles L. Bennett[b], Lance Corbett[b], Haiquan Guo[c], Tobias Marriage[b], Mary Ann B. Meador[d], Karwan Rostem[a], and Edward J. Wollack[a]

[a]NASA Goddard Space Flight Center, Greenbelt, MD 20771 USA
[b]Department of Physics and Astronomy, Johns Hopkins University, Baltimore, MD 21218, USA
[c]Ohio Aerospace Institute, Cleveland, Ohio, 44142, USA
[d]NASA Glenn Research Center, 21000 Brookpark Road, Cleveland, Ohio 44135, United States

ABSTRACT

We present the design and performance of broadband and tunable infrared-blocking filters for millimeter and sub-millimeter astronomy composed of small scattering particles embedded in an aerogel substrate. The ultra-low-density (< 100 mg/cm^3) aerogel substrate provides an index of refraction as low as 1.05, removing the need for anti-reflection coatings and allowing for broadband operation from DC to above 1 THz. The size distribution of the scattering particles can be tuned to provide a variable cutoff frequency. Aerogel filters with embedded high-resistivity silicon powder are being produced at 40-cm diameter to enable large-aperture cryogenic receivers for cosmic microwave background polarimeters, which require large arrays of sub-Kelvin detectors in their search for the signature of an inflationary gravitational-wave background.

Keywords: Cosmic Microwave Background Polarization, Astronomical Optics, Filters, Aerogel

1. INTRODUCTION

Millimeter-wave cryogenic receivers require rejection of infrared (IR) radiation to reduce thermal loads on the cold stages of the cryostat. As telescope apertures increase in diameter to accommodate larger focal planes, the requirements for infrared filtering become more stringent, while the fabrication of filters becomes correspondingly more difficult. This is a particular problem for current cosmic microwave background receivers, which have receiver apertures approaching 1 m in diameter.[1–5] For such large apertures, IR rejection at 1 part in 10^6 is required to enable operation of the focal plane array at sub-Kelvin temperatures.

A variety of approaches have been developed to meet this challenge. Reflective metal-mesh filters, composed of patterned metal films on a thin dielectric substrate, have been widely used.[6–9] Capacitive grids provide strong (> 30 dB) IR rejection with minimal loss at millimeter wavelengths. There are diminishing returns when using multiple reflective filters as reflections from subsequent filters need to transmit through filters further up in the stack to escape the cryostat. Absorptive filters have also been extensively used, in which a material with low loss at millimeter wavelengths but strong absorption in the IR absorbs power and conducts it to higher-temperature stages of a receiver.[10–12] Materials used for this purpose include polytetrafluoroethylene (PTFE), nylon, and alumina. Absorbing filters require anti-reflection coatings and lose effectiveness as their diameter increases, because the centers of the filters tend to heat and re-radiate further down the optical chain. Low-refractive-index foam materials have been used, which scatter and absorb IR power due to their pore size, and then radiate some of that absorbed power back out of the receiver.[13]

We here present the design, fabrication, and performance of highly-transparent, broadband, and tunable IR-blocking filters composed of small scattering particles embedded in an aerogel substrate. They are made to diffusely scatter infrared radiation to a wide range of angles.[14,15] The ultra-low-density (90-200 mc/cm^3) aerogel substrate has a low index of refraction, removing the need for an anti-reflection coating and allowing for

Further author information: (Send correspondence to T. E.-H.)
T. E.-H.: E-mail: thomas.m.essinger-hileman@nasa.gov, Telephone: 1 301-286-3693

Millimeter, Submillimeter, and Far-Infrared Detectors and Instrumentation for Astronomy IX,
edited by Jonas Zmuidzinas, Jian-Rong Gao, Proc. of SPIE Vol. 10708, 107080F
 · doi: 10.1117/12.2313387

ultra-broadband operation across the full range from zero frequency to greater than 10 THz. The size of the scattering particles can be tuned to give variable cutoff frequencies.

Two aerogel materials were investigated for this work: a classic silica aerogel and a flexible and mechanically robust polyimide aerogel. Silica aerogel samples 12 mm × 50 mm × 50 mm were successfully fabricated with densities of 90 mc/cm^3 and silicon loading of 17 and 35 mc/cm^3 with silicon particle size distributions of 60-75 μm and 75-100 μm. Polyimide aerogels were produced in rolls 43 cm × 2 m with thicknesses of 0.3-0.5 mm and silicon loading of 3 and 5 mc/cm^3 with silicon particle size distributions of 50-75 μm and 75-100 μm. Reference samples of unloaded aerogel were produced for both silica and polyimide aerogels.

2. FILTER FABRICATION AND SAMPLE DESCRIPTION

Aerogels are made by supercritical drying of a gel, typically using carbon dioxide. Silicon powder is mixed into the gel before curing and supercritical drying. Silica aerogel samples were produced by Ocellus, Inc.* Polyimide aerogel samples were produced at NASA Glenn Research Center as described in previous publications.[16,17] The polyimide aerogel rolls were produced through a roll-to-roll process, in which the sol was cast to a carrier plastic film in a uniform thickness, allowed to gel, and then dried using supercritical extraction of CO_2.

Sample Number	Dimensions	Aerogel Material	Aerogel Density	Si Particle Sizes	Si Particle Density	Model n	Measured n
	(mm)		(mg/cm^3)	(μm)	(mg/cm^3)		
1	3 x 50 x 50	Silica	90	None	N/A	1.03	1.04
2	3 x 50 x 50	Silica	90	60-75	35	1.04	1.07
3	3 x 50 x 50	Silica	90	60-75	17	1.03	1.06
4	12.5 x 50 x 50	Silica	90	75-100	35	1.04	—†
5	0.3 x 420 x 2000	Polyimide	212	None	N/A	1.09	1.10
6	0.5 x 420 x 2000	Polyimide	178	50-75	3	1.07	1.08
7	0.3 x 420 x 2000	Polyimide	204	75-100	5	1.09	1.13

Table 1. Summary of samples measured. The model assumes index of refraction of 1.7, 2.0, and 3.4 for polyimide, silica, and silicon, respectively. The silicon powder was produced from p-type, boron doped, float-zone silicon wafers with resistivity > 10 kΩ-cm by pulverizing by hand in a mortar and pestle or using a ball milling machine and then sieving to produce powder with a given size distribution.

Silica aerogel samples were initially produced in two base aerogel densities of 50 and 90 mg/cm^3 with a loading of 75-100 μm silicon particles at a density of 35 mg/cm^3. The two initial samples were 50 mm x 50 mm x 12.5 mm in size. The 50 mg/cm^3 sample was found to be too fragile to reliably mount in sample holders for optical measurements, so all further development focused on 90 mg/cm^3 aerogel density. Three further samples were produced and measured with sizes of 50 mm x 50 mm x 3 mm, labeled Samples 1–3, as summarized in Table 2. A reference aerogel was produced with no silicon powder and samples with 17 mg/cm^3 and 35 mg/cm^3 silicon loading density with a particle size distribution of 60–75 μm were produced. The initial thicker sample is labeled Sample 4.

Three polyimide aerogel rolls were produced with a nominal density of 200 mg/cm^3 in sizes approximately 420 mm x 2000 mm and thicknesses in the range 0.3–0.5 mm. Measured values of density are given in Table 2. Sample 5 is a reference sample with no silicon powder, Sample 6 was loaded with 50-75 μm silicon powder, and Sample 7 was loaded with 75–100 μm silicon powder. The addition of silicon powder may decrease shrinkage of the aerogel during supercritical drying, but further investigation is needed to establish this.

*Ocellus, Inc., 450 Lindbergh Avenue, Livermore, CA 94551, information@ocellusinc.com

†High accuracy index of refraction data were not able to be obtained on this thicker sample.

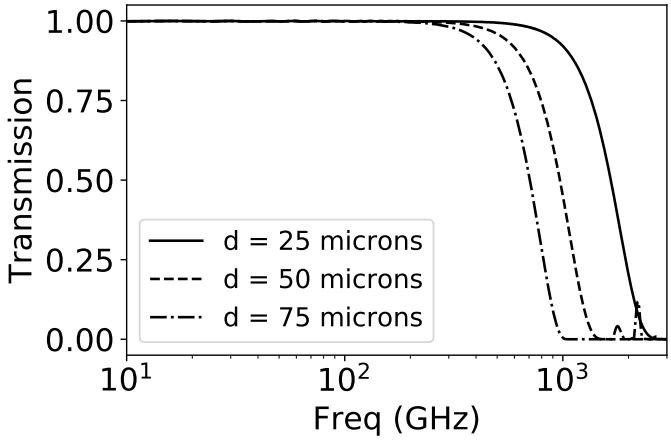

Figure 1. Model estimates of filter transmission versus frequency for 5 mm thick silica aerogel with density of 90 mg/cm^3 (estimated $n = 1.04$) and silicon particles embedded at a density of 35 mg/cm^3 with sizes of 25 μm, 50 μm, and 75 μm, demonstrated the ability to tune the cutoff frequency with particle size.

3. OPTICAL DESIGN

3.1 Low-frequency performance

The filter response is modeled using a combination of effective-dielectric and Mie scattering theory. Example model outputs are shown in Fig. 1. For wavelengths that are large compared to the scattering particle size and separation, the aerogel plus scatterers will behave as a composite material of air, the aerogel matrix material, and silicon. The aerogel without scatterers will have an approximate effective dielectric constant given by Maxwell-Garnett theory[18–20] of:

$$\epsilon_a = \frac{\epsilon_m + 2 + 2f_a\,(\epsilon_m - 1)}{\epsilon_m + 2 - f_a\,(\epsilon_m - 1)}, \tag{1}$$

where ϵ_a and ϵ_m are the dielectric constants of the aerogel and the aerogel matrix material, respectively, and f_a is the volume filling fraction of material in the aerogel. The nanoporous structure of typical aerogels allows them to behave like effective dielectrics well into the infrared and on length scales associated with the scattering particles used in this work (> 1 μm).

The inclusion of a small filling fraction of scattering particles increases the dielectric constant. For the small filling fractions ($\lesssim 1\%$) used in the scattering filters, it is valid to calculate an effective dielectric constant for the base aerogel and then use Maxwell-Garnett theory again to calculate a new effective dielectric constant

$$\bar{\epsilon} = \epsilon_a \frac{\epsilon_s + 2\epsilon_a + 2f_s\,(\epsilon_s - \epsilon_a)}{\epsilon_s + 2\epsilon_a - f_s\,(\epsilon_s - \epsilon_a)}, \tag{2}$$

where ϵ_a is the aerogel dielectric constant calculated from Eq. 1, ϵ_s is that of the scattering particles, and f_s is the volume filling fraction of the scattering particles in the medium.

The reflection at normal incidence for such a film with a thickness t is calculated in standard texts:[21]

$$R = \frac{2r^2\,(1 + \cos 2\beta)}{1 + r^4 + 2r^2 \cos 2\beta}, \tag{3}$$

where $r = (\bar{n} - 1)/(\bar{n} + 1)$ for $\bar{n} = \sqrt{\mathrm{Re}(\bar{\epsilon})}$ and $\beta = 2\pi\nu\bar{n}t/c$ is the phase delay in the material at frequency ν. For small r, the total reflectance exhibits fringes between 0 and $4r^2$. The aerogels in this study have indices

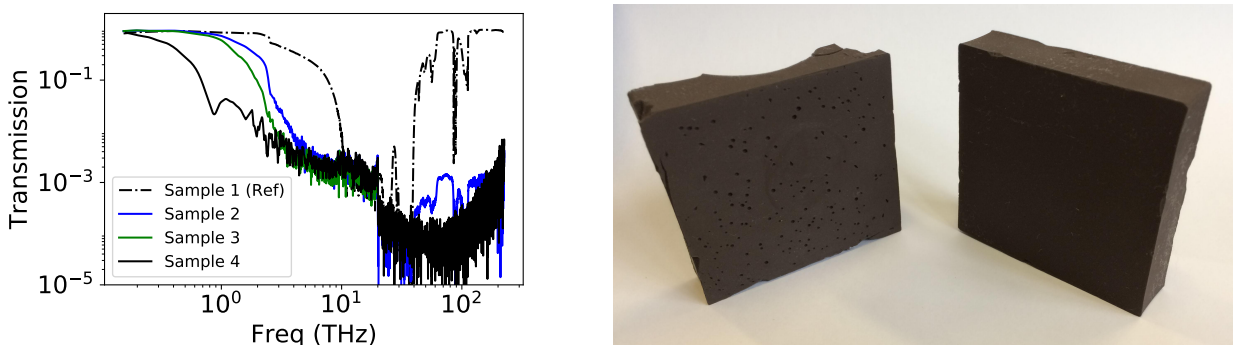

Figure 2. *Left:* Transmission spectra of 90 mg/cm^3 silica aerogel with no silicon powder (dot-dash black), with 17 mg/cm^3 (blue) and 35 mg/cm^3 (green) of 60-75 μm silicon particles, and with 35 mc/cm^3 of 75-100 μm silicon particles (solid black). Samples were approximately 3 mm thick. Measurements below 1.5 THz were made with a time-domain THz spectrometer, while measurements at higher frequencies were made with a Bruker Fourier transform spectrometer. *Right:* Photographs of two silicon-loaded silica aerogel samples of different silica density. The left sample has density of 50 mg/cm^3 and the right sample 90 mg/cm^3.

of refraction in the range 1.04-1.13. For a material in the middle of this range with $\bar{n} = 1.10$, the maximum reflectance is 0.9% and the average reflectance across all frequencies is $< 0.5\%$. Judicious choice of filter thickness for a given observing band can reduce reflections from the filter to levels of 0.1%.

The samples show measured indices of refraction above that predicted from Maxwell-Garnett theory given the bulk properties of silica, polyimide, and silicon alone. This may indicate a difference between the bulk properties and the properties of the materials in the gel matrix or the presence of other adsorbed materials, such as water, facilitated by the high pore surface area of the aerogels.

3.2 Scattering at high frequency

Optical scattering theory has been developed extensively in the literature.[22,23] The scattering of light from spherical particles can be solved analytically.[24] The scattered intensity can be expanded as a sum of Bessel functions and depends on the ratio between the size of the spherical particle and the wavelength of light, as well as the scattered direction and indices of refraction of the medium and the scatterers. For a medium containing many small scatterers, transmission through the medium can be shown to depend solely on the forward-scattered amplitude, $Q_{\rm sca}$. See Appendix A for further details.

The specific intensity of light passing through a medium of scatterers is attenuated as

$$I(z) = I_0 \exp\left(-N\pi a^2 Q_{\rm sca} z\right) = I_0 \exp\left(-\gamma z\right), \tag{4}$$

where N is the volume density of scatterers, a is the particle radius, and z is the distance traveled through the medium. The attenuation coefficient has been defined as $\gamma = N\pi a^2 Q_{\rm sca}$.

The attenuation through a scattering medium with a distribution of sizes can be straightforwardly handled by integrating over the particle size. If the number of scatterers per unit volume is a function of particle radius, $N(a)$, then the attenuation coefficient is

$$\gamma = \int_0^\infty N(a)\pi a^2 Q_{\rm sca}(r) dr. \tag{5}$$

Using this model, we are able to estimate the frequency cutoff of our filters in the limits that:

1. The particles are roughly spherical. This is not strictly true, but is a reasonable first approximation for randomly-oriented nearly-spherical particles and is particularly relevant for long wavelengths.
2. Scattering is not strong enough for multiple scattering events to play a significant role.

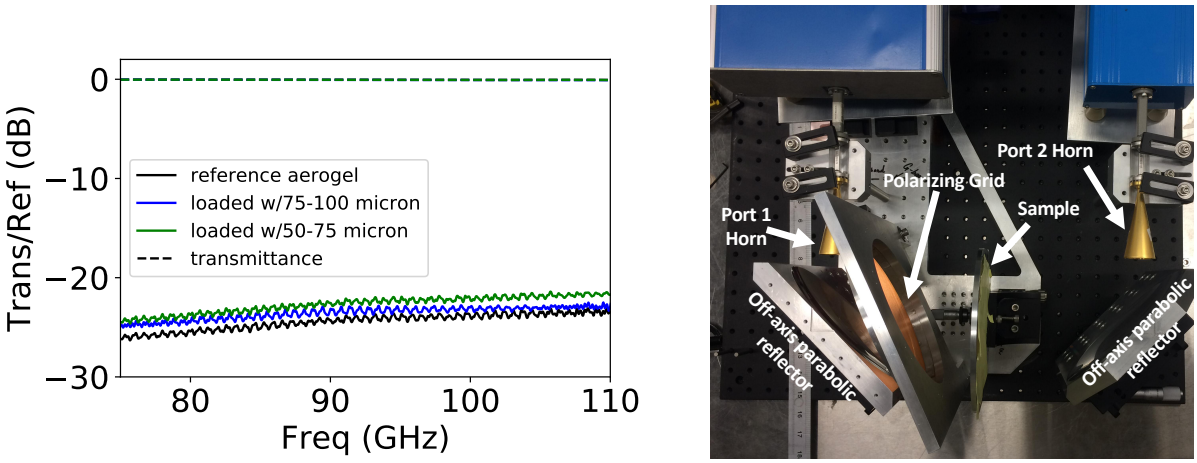

Figure 3. *Left:* Vector network analyzer measurements of the reflectance (solid lines) and transmittance (dashed lines) of polyimide aerogel samples with no silicon powder (black), 3 mc/cm^3 of 50-75 μm silicon powder (green), and 5 mc/cm^3 of 75-100 μm silicon powder (blue). *Right:* Photograph of the setup used to make the measurements. Scalar feedhorns both transmit and receive power through the system. Off-axis parabolic reflectors provide a beam waist at approximately the location of the sample and a polarizing wiregrid reduces mode coupling in the setup. The sample is mounted on a linear translation stage.

3.3 Integrated Model

The complex dielectric constant estimated from Maxwell-Garnett theory in Sec. 3.1 can be combined with the additional attenuation, γ, estimated from Mie scattering theory in Sec. 3.2. The attenuation due to scattering contributes to the complex part of the dielectric constant to give a total effective dielectric constant of

$$\epsilon_{eff} = \mathrm{Re}(\bar{\epsilon}) + \imath \left(\mathrm{Im}(\bar{\epsilon}) + \frac{c\gamma}{2\pi\bar{n}\nu} \right). \tag{6}$$

This dielectric constant can then be incorporated into a transfer-matrix code for calculation of the expected transmission spectrum of a given filter. An example of model outputs for silica aerogel filters 5 mm thick with silicon particles embedded at a density of 35 mg/cm^3 of three different sizes (25 μm, 50 μm, and 75 μm) is shown in Fig. 1. We note that because our particles are not spherical and multiple scattering plays a role at high frequencies, the model does not reproduce filter response in great details. Rather the model is used to guide filter design to choose appropriate particle size and loading volume percentage to achieve a desired cutoff frequency.

4. MEASUREMENTS

Transmission and reflection data were taken of samples to evaluate their performance. The silica aerogel samples were measured in transmission using a time-domain THz spectroscopy system[25] for frequencies 0.15–1.5 THz and a Bruker FTS for transmission at frequencies of 1.5–200 THz. Polyimide aerogel samples were measured using a Bruker FTS for infrared transmission across frequencies 1–18 THz and a quasi-optical vector network analyzer (VNA) setup for reflection at W band (75-110 GHz). VNA reflectance measurements were taken multiple (~ 5) times with sample positions translated by approximately $\lambda/5$ each time, following the method outlined in Ref. 26.

Silica aerogel filters were mounted in holders with 8 mm diameter apertures after being cut to size with a diamond wire saw. Stycast 2850 epoxy was mixed and allowed to get tacky before application, as it was found that otherwise the epoxy wicked into the aerogel samples and caused fracturing. Polyimide aerogel samples were mounted on sample holders with aperture diameters of 125 mm for VNA measurements and 12.5 mm for FTS measurements using double-sided pressure-sensitive adhesive tape.

Figure 2 shows transmission spectra and photographs of silica aerogel samples. The transmission spectra demonstrate high transmission at millimeter wavelengths, rejection of IR power at > 25 dB, and a tunable cutoff

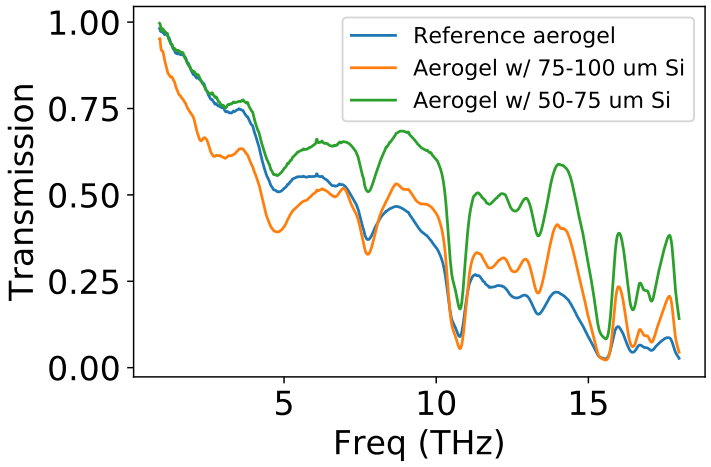

Figure 4. *Left:* Measurements of IR transmission of polyimide aerogel samples with a Bruker FTS. Measurements were taken with a 12.5 mm diameter aperture for samples with no silicon powder (blue), 5 mg/cm^3 silicon powder with size distribution 75–100 μm (orange), and 3 mg/cm^3 silicon powder with size distribution 50–75 μm (green). *Right:* Photograph of a polyimide aerogel roll, approximately 420 mm wide.

frequency by choice of silicon loading density and particle size distribution. Figure 3 summarizes measurements of polyimide aerogel samples with the VNA setup, demonstrating high transmission ($> 99\%$) and low reflection (~ -25 dB or 0.3%) at W band. Figure 4 shows FTS transmission spectra in the IR across the range 1–18 THz for the three polyimide samples, along with a photograph of one of the polyimide aerogel rolls. The FTS IR transmission data highlight the need for further investigation of filters with higher silicon powder loading and lower IR absorption.

5. CONCLUSION

We have fabricated infrared blocking filters composed of ultra-low index of refraction aerogel substrates with embedded silicon scattering particles. Both silica and polyimide aerogel filters were fabricated and tested for transmission and reflection at millimeter and far-IR wavelengths. We have demonstrated the ability of aerogel scattering filters to have (1) high ($> 99\%$) transmission across an ultra-broad bandwidth from DC to 1 THz or higher, (2) > 25 dB rejection of IR power, and (3) a cutoff frequency that is tunable through choice of silicon particle size and loading density.

6. ACKNOWLEDGEMENTS

We acknowledge the National Science Foundation Division of Astronomical Sciences for their support of this work under Grant Numbers 0959349, 1429236, 1636634, and 1654494, as well as the National Aeronautics and Space Administration under grant number NNX14AB76A. We would like to thank Dipanjan Chaudhuri and others in the Armitage lab at Johns Hopkins University for making measurements of silica aerogel filter samples; Ocellus Inc. for providing silica aerogel samples; and Kevin Miller and Alyssa Barliss in the Optics Branch at GSFC for FTS measurements of polyimide aerogel samples. T. E.-H. was funded by a National Science Foundation Astronomy and Astrophysics Postdoctoral Fellowship.

APPENDIX A. SCATTERING THEORY

As developed in Refs. 22, 23, for spherical particles $Q_{\rm sca}$ is given by

$$Q_{\rm sca} = \frac{2}{x^2}\sum_{n=1}^{\infty}(2n+1)\left(|a_n|^2+|b_n|^2\right), \tag{7}$$

where $x = 2\pi a/\lambda$ is the size parameter that depends on the radius of the particle, a, and the wavelength of the light, λ. The coefficients a_n and b_n are given in terms of Riccati-Bessel functions as

$$a_n = \frac{\Psi_n'(mx)\Psi_n(x) - m\Psi_n(mx)\Psi_n'(x)}{\Psi_n'(mx)\zeta_n(x) - m\Psi_n(mx)\zeta_n'(x)} \tag{8}$$

and

$$b_n = \frac{m\Psi_n'(mx)\Psi_n(x) - \Psi_n(mx)\Psi_n'(x)}{m\Psi_n'(mx)\zeta_n(x) - \Psi_n(mx)\zeta_n'(x)}. \tag{9}$$

Primes denote derivatives with respective to x, and the functions Ψ_n and ζ_n are written in terms of Bessel functions of the first kind, J_n, and Hankel functions of the second kind, $H_n^{(2)}$,

$$\begin{aligned}\Psi_n(x) &= \left(\tfrac{\pi x}{2}\right)^{1/2} J_{n+1/2}(x);\\ \zeta_n(x) &= \left(\tfrac{\pi x}{2}\right)^{1/2} H^{(2)}_{n+1/2}(x).\end{aligned} \tag{10}$$

REFERENCES

[1] Essinger-Hileman, T., Ali, A., Amiri, M., Appel, J. W., Araujo, D., Bennett, C. L., Boone, F., Chan, M., Cho, H.-M., Chuss, D. T., Colazo, F., Crowe, E., Denis, K., Dünner, R., Eimer, J., Gothe, D., Halpern, M., Harrington, K., Hilton, G. C., Hinshaw, G. F., Huang, C., Irwin, K., Jones, G., Karakla, J., Kogut, A. J., Larson, D., Limon, M., Lowry, L., Marriage, T., Mehrle, N., Miller, A. D., Miller, N., Moseley, S. H., Novak, G., Reintsema, C., Rostem, K., Stevenson, T., Towner, D., U-Yen, K., Wagner, E., Watts, D., Wollack, E. J., Xu, Z., and Zeng, L., "CLASS: the cosmology large angular scale surveyor," in [*Millimeter, Submillimeter, and Far-Infrared Detectors and Instrumentation for Astronomy VII*], *Proceedings of SPIE* **9153**, 91531I (July 2014).

[2] Benson, B. A., Ade, P. A. R., Ahmed, Z., Allen, S. W., Arnold, K., Austermann, J. E., Bender, A. N., Bleem, L. E., Carlstrom, J. E., Chang, C. L., Cho, H. M., Cliche, J. F., Crawford, T. M., Cukierman, A., de Haan, T., Dobbs, M. A., Dutcher, D., Everett, W., Gilbert, A., Halverson, N. W., Hanson, D., Harrington, N. L., Hattori, K., Henning, J. W., Hilton, G. C., Holder, G. P., Holzapfel, W. L., Irwin, K. D., Keisler, R., Knox, L., Kubik, D., Kuo, C. L., Lee, A. T., Leitch, E. M., Li, D., McDonald, M., Meyer, S. S., Montgomery, J., Myers, M., Natoli, T., Nguyen, H., Novosad, V., Padin, S., Pan, Z., Pearson, J., Reichardt, C., Ruhl, J. E., Saliwanchik, B. R., Simard, G., Smecher, G., Sayre, J. T., Shirokoff, E., Stark, A. A., Story, K., Suzuki, A., Thompson, K. L., Tucker, C., Vanderlinde, K., Vieira, J. D., Vikhlinin, A., Wang, G., Yefremenko, V., and Yoon, K. W., "SPT-3G: a next-generation cosmic microwave background polarization experiment on the South Pole telescope," in [*Millimeter, Submillimeter, and Far-Infrared Detectors and Instrumentation for Astronomy VII*], *Proceedings of SPIE* **9153**, 91531P (July 2014).

[3] Grayson, J. A., Ade, P. A. R., Ahmed, Z., Alexander, K. D., Amiri, M., Barkats, D., Benton, S. J., Bischoff, C. A., Bock, J. J., Boenish, H., Bowens-Rubin, R., Buder, I., Bullock, E., Buza, V., Connors, J., Filippini, J. P., Fliescher, S., Halpern, M., Harrison, S., Hilton, G. C., Hristov, V. V., Hui, H., Irwin, K. D., Kang, J., Karkare, K. S., Karpel, E., Kefeli, S., Kernasovskiy, S. A., Kovac, J. M., Kuo, C. L., Leitch, E. M., Lueker, M., Megerian, K. G., Monticue, V., Namikawa, T., Netterfield, C. B., Nguyen, H. T., O'Brient, R., Ogburn, R. W., Pryke, C., Reintsema, C. D., Richter, S., Schwarz, R., Sorenson, C., Sheehy, C. D., Staniszewski,

Z. K., Steinbach, B., Teply, G. P., Thompson, K. L., Tolan, J. E., Tucker, C., Turner, A. D., Vieregg, A. G., Wandui, A., Weber, A. C., Wiebe, D. V., Willmert, J., Wu, W. L. K., and Yoon, K. W., "BICEP3 performance overview and planned Keck Array upgrade," in [*Millimeter, Submillimeter, and Far-Infrared Detectors and Instrumentation for Astronomy VIII*], *Proceedings of SPIE* **9914**, 99140S (July 2016).

[4] Suzuki, A., Ade, P., Akiba, Y., Aleman, C., Arnold, K., Baccigalupi, C., Barch, B., Barron, D., Bender, A., Boettger, D., Borrill, J., Chapman, S., Chinone, Y., Cukierman, A., Dobbs, M., Ducout, A., Dunner, R., Elleflot, T., Errard, J., Fabbian, G., Feeney, S., Feng, C., Fujino, T., Fuller, G., Gilbert, A., Goeckner-Wald, N., Groh, J., Haan, T. D., Hall, G., Halverson, N., Hamada, T., Hasegawa, M., Hattori, K., Hazumi, M., Hill, C., Holzapfel, W., Hori, Y., Howe, L., Inoue, Y., Irie, F., Jaehnig, G., Jaffe, A., Jeong, O., Katayama, N., Kaufman, J., Kazemzadeh, K., Keating, B., Kermish, Z., Keskitalo, R., Kisner, T., Kusaka, A., Jeune, M. L., Lee, A., Leon, D., Linder, E., Lowry, L., Matsuda, F., Matsumura, T., Miller, N., Mizukami, K., Montgomery, J., Navaroli, M., Nishino, H., Peloton, J., Poletti, D., Puglisi, G., Rebeiz, G., Raum, C., Reichardt, C., Richards, P., Ross, C., Rotermund, K., Segawa, Y., Sherwin, B., Shirley, I., Siritanasak, P., Stebor, N., Stompor, R., Suzuki, J., Tajima, O., Takada, S., Takakura, S., Takatori, S., Tikhomirov, A., Tomaru, T., Westbrook, B., Whitehorn, N., Yamashita, T., Zahn, A., and Zahn, O., "The Polarbear-2 and the Simons Array Experiments," *Journal of Low Temperature Physics* **184**, 805–810 (Aug. 2016).

[5] Thornton, R. J., Ade, P. A. R., Aiola, S., Angilè, F. E., Amiri, M., Beall, J. A., Becker, D. T., Cho, H.-M., Choi, S. K., Corlies, P., Coughlin, K. P., Datta, R., Devlin, M. J., Dicker, S. R., Dünner, R., Fowler, J. W., Fox, A. E., Gallardo, P. A., Gao, J., Grace, E., Halpern, M., Hasselfield, M., Henderson, S. W., Hilton, G. C., Hincks, A. D., Ho, S. P., Hubmayr, J., Irwin, K. D., Klein, J., Koopman, B., Li, D., Louis, T., Lungu, M., Maurin, L., McMahon, J., Munson, C. D., Naess, S., Nati, F., Newburgh, L., Nibarger, J., Niemack, M. D., Niraula, P., Nolta, M. R., Page, L. A., Pappas, C. G., Schillaci, A., Schmitt, B. L., Sehgal, N., Sievers, J. L., Simon, S. M., Staggs, S. T., Tucker, C., Uehara, M., van Lanen, J., Ward, J. T., and Wollack, E. J., "The Atacama Cosmology Telescope: The Polarization-sensitive ACTPol Instrument," *ApJS* **227**, 21 (Dec. 2016).

[6] Ulrich, R., "Far-infrared properties of metallic mesh and its complementary structure," *Infrared Physics* **7**, 37–50 (Mar. 1967).

[7] Ulrich, R., "Effective low-pass filters for far infrared frequencies," *Infrared Physics* **7**, 65–74 (June 1967).

[8] Whitbourn, L. B. and Compton, R. C., "Equivalent-circuit formulas for metal grid reflectors at a dielectric boundary," *OSA* **24**, 217–220 (Jan. 1985).

[9] Ade, P. A. R., Pisano, G., Tucker, C., and Weaver, S., "A review of metal mesh filters," in [*Society of Photo-Optical Instrumentation Engineers (SPIE) Conference Series*], *Society of Photo-Optical Instrumentation Engineers (SPIE) Conference Series* **6275** (July 2006).

[10] Halpern, M., Gush, H. P., Wishnow, E., and Cosmo, V. D., "Far infrared transmission of dielectrics at cryogenic and room temperatures: glass, fluorogold, eccosorb, stycast, and various plastics," *Appl. Opt.* **25**, 565–570 (Feb 1986).

[11] Bock, J. J. and Lange, A. E., "Performance of a low-pass filter for far-infrared wavelengths," *Appl. Opt.* **34**, 7254–7257 (Nov 1995).

[12] Munson, C. D., Choi, S. K., Coughlin, K. P., McMahon, J. J., Miller, K. H., Page, L. A., and Wollack, E. J., "Composite reflective/absorptive ir-blocking filters embedded in metamaterial antireflection-coated silicon," *Appl. Opt.* **56**, 5349–5354 (Jul 2017).

[13] Choi, J., Ishitsuka, H., Mima, S., Oguri, S., Takahashi, K., and Tajima, O., "Radio-transparent multi-layer insulation for radiowave receivers," *Review of Scientific Instruments* **84**, 114502–114502–6 (Nov. 2013).

[14] DeVore, J. R. and Pfund, A. H., "Optical scattering by dielectric powders of uniform particle size∗," *J. Opt. Soc. Am.* **37**, 826–832 (Oct 1947).

[15] Plummer, J. H., "Transmissions of powder films to the infrared spectrum," *J. Opt. Soc. Am.* **26**, 434–438 (Dec 1936).

[16] Meador, M. A. B., Malow, E. J., Silva, R., Wright, S., Quade, D., Vivod, S. L., Guo, H., Guo, J., and Cakmak, M., "Mechanically strong, flexible polyimide aerogels cross-linked with aromatic triamine," *ACS Applied Materials & Interfaces* **4**, 536–544 (jan 2012).

[17] Meador, M. A. B., Wright, S., Sandberg, A., Nguyen, B. N., Keuls, F. W. V., Mueller, C. H., Rodríguez-Solís, R., and Miranda, F. A., "Low dielectric polyimide aerogels as substrates for lightweight patch antennas," *ACS Applied Materials & Interfaces* **4**, 6346–6353 (nov 2012).

[18] Garnett, J. C. M., "Colours in metal glasses and in metallic films," *Philosophical Transactions of the Royal Society of London A: Mathematical, Physical and Engineering Sciences* **203**(359-371), 385–420 (1904).

[19] Niklasson, G. A., Granqvist, C. G., and Hunderi, O., "Effective medium models for the optical properties of inhomogeneous materials," *Appl. Opt.* **20**, 26–30 (Jan 1981).

[20] Sihvola, A., [*Electromagnetic Mixing Formulas and Applications*], Institution of Engineering and Technology, London, United Kingdom, Electromagnetic Wave Series ed. (2008).

[21] Born, M. and Wolf, E., [*Principles of Optics*] (Oct. 1999).

[22] van de Hulst, H. C., [*Light Scattering by Small Particles*] (1957).

[23] Bohren, C. F. and Huffman, D. R., [*Absorption and scattering of light by small particles*] (1983).

[24] Mie, G., "Beiträge zur Optik trüber Medien, speziell kolloidaler Metallösungen," *Annalen der Physik* **330**, 377–445 (1908).

[25] Morris, C. M., Aguilar, R. V., Stier, A. V., and Armitage, N. P., "Polarization modulation time-domain terahertz polarimetry," *Optics Express* **20**, 12303 (May 2012).

[26] Eimer, J. R., Bennett, C. L., Chuss, D. T., and Wollack, E. J., "Note: Vector reflectometry in a beam waveguide," *Review of Scientific Instruments* **82**, 086101–086101 (Aug. 2011).